Journal of Applied Polymer Science

Poly(Acrylic Acid-*co*-Acrylamide-*co*-2-Acrylamido-2-Methyl-1-Propanesulfonic Acid)-Grafted Nanocellulose/Poly(Vinyl Alcohol) Composite for the *In Vitro* Gastrointestinal Release of Amoxicillin

Thayyath Sreenivasan Anirudhan, Sylaja Raveendran Rejeena
Department of Chemistry, University of Kerala, Kariavattom, Trivandrum, 695581, India
Correspondence to: T. S. Anirudhan (E-mail: tsani@rediffmail.com)

ABSTRACT: Superabsorbent polymer composites (SAPCs) are very promising and versatile materials for biomedical applications. This study concentrates on the development of novel cellulose-based SAPC, Poly(acrylic acid-*co*-acrylamide-*co*−2-acrylamido-2-methyl-1-propanesulfonic acid)-grafted nanocellulose/poly(vinyl alcohol) composite, P(AA-*co*-AAm-*co*-AMPS)-*g*-NC/PVA, as a potential drug delivery vehicle. Amoxicillin was selected as a model drug, which is used for the treatment of *Helicobacter pylori* induced peptic and duodenal ulcers. P(AA-*co*-AAm-*co*-AMPS)-*g*-NC/PVA was synthesized by graft copolymerization reaction, and FTIR, XRD, SEM, and DLS analyses were performed for its characterization. Equilibrium swelling studies were conducted to evaluate the stimuli-response behavior of the SAPC and found that equilibrium swelling was dependent on pH, contact time, temperature, ionic strength, concentration of crosslinker and PVA. Maximum drug encapsulation efficiency was found out by using different concentrations of amoxicillin. Drug release studies were carried out at simulated gastric and intestinal fluids and the release % was observed as maximum in intestinal fluids within 4 h. The drug release kinetics was investigated using Peppas' potential equation and follows non-Fickian mechanism at pH 7.4. Thus, the drug release experiments indicate that P(AA-*co*-AAm-*co*-AMPS)-*g*-NC/PVA would be a fascinating vehicle for the *in vitro* administration of amoxicillin into the gastrointestinal tract. © 2014 Wiley Periodicals, Inc. J. Appl. Polym. Sci. **2014**, *131*, 40699.

KEYWORDS: addition polymerization; biocompatibility; biodegradable; cellulose and other wood products; composites

Received 23 December 2013; accepted 4 March 2014
DOI: 10.1002/app.40699

INTRODUCTION

Drug delivery is a field of vital importance to medicine and healthcare. New drug delivery systems are needed to deliver therapeutic molecules and to improve the therapeutic efficacy and safety of drugs administered. The therapeutic molecules like antibiotics and antibacterial agents are widely administered into the body by conventional method. Amoxicillin (AMO), a semi-synthetic antiobiotic belonging to the β-lactam family, is effective for bacterial infection treatment; especially for *Helicobacter pylori* infection.[1] *Helicobacter pylori* is a causative agent in chronic active gastritis, gastric and duodenal ulcers and gastric adenocarcinoma.[2] *Helicobacter pylori* have the capacity to penetrate the gastric mucus layer and fix itself to various phospholipids and glycolipids in the mucus gel.[3] Therefore, site specific delivery of antimicrobial agents only to the gastrointestinal region will be beneficial. Also, it is reported that the small intestine is the primary site for drug absorption and therefore the gastrointestinal tract is a preferred area to target with various controlled devices. AMO can be delivered into the different parts of human body, especially in the gastrointestinal regions, as reported in previous literatures. Nagahara et al. formulated AMO in the form of mucoadhesive microspheres by spray chilling method, which have the ability to reside in the gastrointestinal tract for an extended period.[4] Improved gastric mucoadhesion was achieved with modified positively charged biodegradable microspheres of amoxicillin, prepared by Wang et al.[5] Liu et al. prepared mucoadhesive microspheres containing AMO and about 90 % was released in the acidic medium within 4 h.[6]

However, conventional drug delivery systems (DDS) are unable to deliver the antibiotics to the site of infection in effective concentration and in fully active forms. Controlled DDS, which are capable of delivering drugs at predetermined rates for predefined periods of time, have been used to overcome the shortcoming of conventional drug formulations. Controlled DDS provide a therapeutic quality of medicines to the proper site in

the body in order to achieve the desired effect with minimum toxicity.

Drug delivery systems must be biocompatible, nontoxic and have the capability to release the drug or bioactive agents to the desired site of action.[7] Polymeric controlled delivery system is the most simplest of controlled drug delivery system. This system is more advantageous and differs from conventional systems by the way in which they disintegrate and their sensitivity to the change in metabolic stage.[8] Natural polymers such as cellulose are used for various biomedical applications, owing to their biodegradable nature. Cellulosics are appealing hydrogel precursor materials, due to their low cost, the large availability and biocompatibility of cellulose, and the responsiveness of cellulosics to variations of external stimuli.[9] Controlled release through oral delivery is usually based on the strong pH-variations and cellulose-based polyelectrolyte hydrogels are particularly suitable for this application.[10] Nanocellulose (NC) is hydrophilic as compared to cellulose and can make use for the preparation of hydrogels due to the large number of hydroxyl groups exposed to surface. Polyvinyl alcohol (PVA) has long been used with other natural polymers because of PVA's ability to form films. PVA is readily soluble in water and exhibits excellent water retention properties. PVA is an odorless and nontoxic polymer. PVA is also susceptible to biological degradation, even though the process is slow.[11] The combination of PVA with other cheap renewable polymers such as cellulose and starch will improve its biodegradation rate and lower the overall cost.[12] The composites based on NC and PVA show improved physical properties compared to individual ones.[13,14] Since NC and PVA molecules have a large number of hydroxyl groups, NC/PVA composites may display a hydrophilic nature. Because of their higher degree of water absorbancy, they are usually biocompatible in nature and are nonirritating to the soft tissues when in contact with them. The hydrophilicity, mechanical strength, thermal stability, and pH-sensitivity of the material can further be improved by graft copolymerization reaction which tailors desired functionalities in the polymer. The graft copolymerized polymers are proven to be effective candidates for making drug delivery systems since it prevents burst release and controls the release of drugs in a prolonged manner.

The aim of this study is to develop a special drug release matrix in gastrointestinal region. Considering this aim, we have prepared a novel superabsorbent composite, poly(acrylic acid-*co*-acrylamide-*co*-2-acrylamido-2-methyl-1-propanesulfonic acid)-grafted nanocellulose/poly(vinyl alcohol) composite [P(AA-*co*-AAm-*co*-AMPS)-*g*-NC/PVA]. P(AA-*co*-AAm-*co*-AMPS)-*g*-NC/PVA was synthesized by graft copolymerization reaction of a mixture of acrylic acid (AA), acrylamide (AAm), and 2-acrylamido-2-methyl-1-propanesulfonic acid (AMPS) onto nanocellulose/poly(vinyl alcohol) composite in the presence of *N,N*'-methylenebisacrylamide (MBA) as a cross-linking agent and potassium persulfate ($K_2S_2O_8$) as a free radical initiator. The presence of AA, AMPS in the polymer chain may create a large number of ionizable $–COO^-$ and $-SO_3^{--}$ groups respectively, which may increase the swelling capacity and drug encapsulation efficiency. Also, the hydrogels made of polyanions can be used to develop formulations that release drugs in a neutral pH environment.[15] The swelling and pH responsiveness of polyelectrolyte hydrogels can be adjusted by using neutral commoners, like acrylamide, methyl methacrylate, 2-hydroxyethyl methacrylate, and maleic anhydride.[16] The presence of different comonomers in a polymer chain provides different hydrophobicity, leading to unique pH-sensitive behavior.

In this work, we have synthesized a novel DDS, P(AA-*co*-AAm-*co*-AMPS)-*g*-NC/PVA for the controlled *in vitro* release of AMO into the gastrointestinal tract. The swelling capacity and drug encapsulation efficiency of the P(AA-*co*-AAm-*co*-AMPS)-*g*-NC/PVA was optimized from different conditions. A delayed drug release was observed while analyzing the *in vitro* drug release data and the drug release was found to be easier in intestine rather than gastric region. Thus the newly developed drug carrier, P(AA-*co*-AAm-*co*-AMPS)-*g*-NC/can be used for the eradication of *Helicobacter pylori*.

EXPERIMENTAL

Materials

For the extraction of Cellulose, saw dust of Mangiferra indica (collected from Local saw mill, Trivandrum) was used after thorough washing and drying at 80°C. PVA ($M_W = 125{,}000$ g/mol) was obtained from SD Fine Chem (Mumbai, India). Amoxcillin trihydrate (AMO) was purchased from Fluka, Switzerland. Acrylic acid (AA), acrylamide (AAm) and 2-acrylamido-2-methyl-1-propanesulfonic acid (AMPS) were obtained from Sigma-Aldrich, Milwau-kee, WI. *N,N*'-methylenebisacrylamide (MBA), potassium persulfate ($K_2S_2O_8$), potassium chloride, hydrochloric acid, disodium hydrogen phosphate (Na_2HPO_4), potassium dihydrogen phosphate (KH_2PO_4), and sodium hydroxide were purchased from E-Merck (Worli, Mumbai, India) and used without further purification. Distilled water was used throughout the study.

Preparation of P(AA-co-AAm-co-AMPS)-g-NC/PVA

The general procedure adopted for the synthesis of P(AA-*co*-AAm-*co*-AMPS)-*g*-NC/PVA is presented in Scheme 1. The synthesis involves the following steps.

Step 1. Extraction of Cellulose from Saw Dust. Saw dust was pretreated with 10% H_2SO_4 solution (120○C, 10 min) and centrifuged to remove rich pentosanes solution. Delignification was achieved by the subsequent treatment with 1% NaOH (100°C, 1 h). The obtained brown mass was bleached with 5% H_2O_2 (80○C, 1 h) yielded white cellulose as the product.

Step 2. Preparation of Nanocellulose (NC) from Cellulose. About 5 g of cellulose was dispersed in 250 mL distilled water under magnetic stirring (20 min). 140 mL 98 % sulfuric acid was dropped to the homogenized mixture, without cause heating. After complete addition, the mixture was heated at 50○C for 2 h. The hot mixture was diluted ten times with ice cooled distilled water. The obtained white colloid was centrifuged, washed many times with water, and freeze-dried.[17]

Step 3. Synthesis of P(AA-co-AAm-co-AMPS)-g-NC/PVA. P(AA-*co*-AAm-*co*-AMPS)-*g*-NC/PVA was synthesized by the graft copolymerization reaction of AA, AAm, and AMPS onto NC/PVA composite in the presence of MBA as a crosslinking

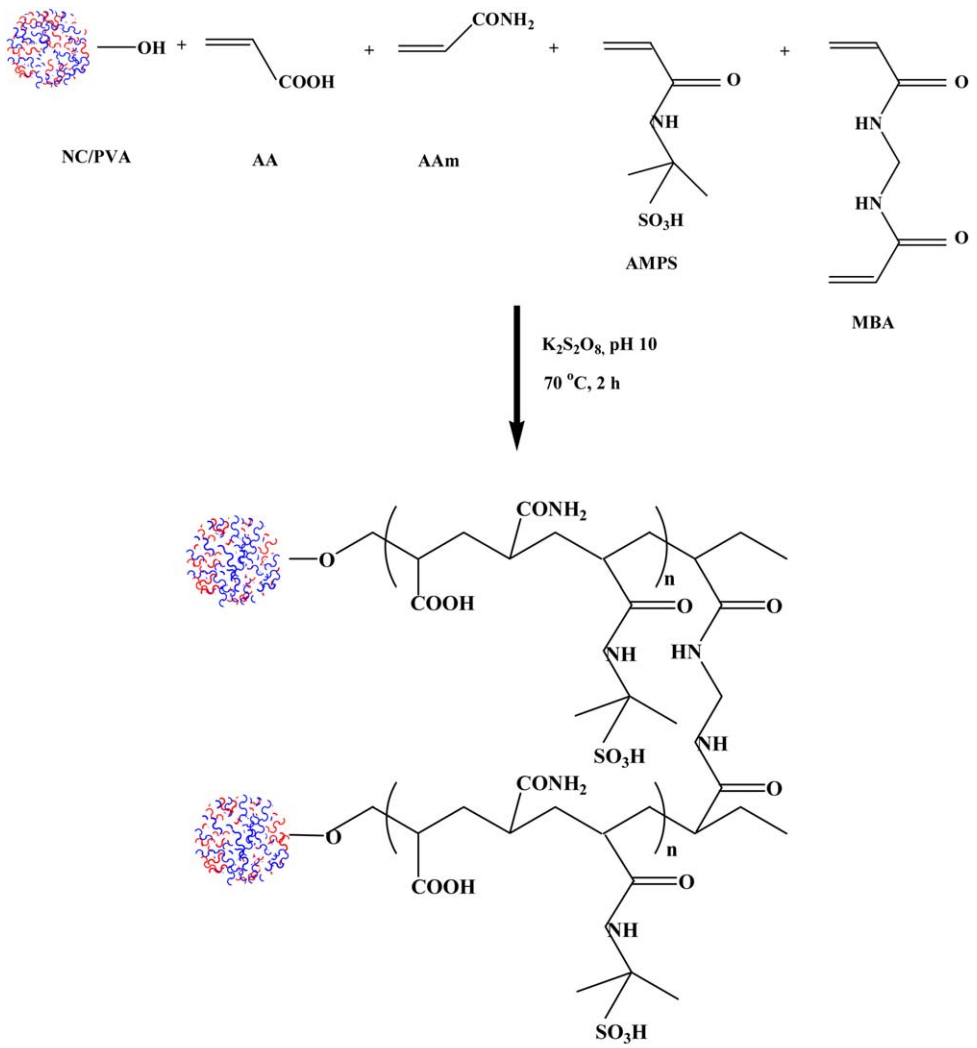

Scheme 1. Expected reaction mechanism for the synthesis of P(AA-*co*-AAm-*co*-AMPS)-*g*-NC/PVA. [Color figure can be viewed in the online issue, which is available at wileyonlinelibrary.com.]

agent and $K_2S_2O_8$ as a free radical initiator. Typically, PVA (0.1–1.0 g) was dissolved in 200 mL distilled water and added NC (1.0 g) under magnetic stirring (70○C, 1 h). To the obtained NC/PVA composite, $K_2S_2O_8$ (0.46 g; initiator) was added and kept at 60○C for 10 min. After cooling the suspension to 40○C, a mixture of AA (0.05*M*, 3.4 mL), AAm (0.05*M*, 3.6 g), AMPS (0.05*M*, 9.4 mL), and MBA (1.16 g; crosslinker) were added. The pH was adjusted by NaOH to 10.0. The temperature was raised to 70○C and maintained for 2 h to complete the reaction. The obtained product was filtered and washed repeatedly with distilled water and ethanol to remove homopolymers. The product, P(AA-*co*-AAm-*co*-AMPS)-*g*-NC/PVA was dried in an air oven by keeping the temperature at 50○C for 6 h and stored in vacuum for further use.

Determination of Sulfonyl and Carboxyl Groups

The total amount of acidic groups present in P(AA-*co*-AAm-*co*-AMPS)-*g*-NC/PVA can be determined as follows. About 50 mg of the sample is taken in a 100 mL stoppered bottle. Added 20 mL 0.01*M* NaCl solution and shaken for 1 h. Filtered the solution and the filtrate was titrated against 0.01*M* NaOH solution using phenolphthalein as indicator. Boehm titration was performed to estimate the -COOH functional groups present in P(AA-*co*-AAm-*co*-AMPS)-*g*-NC/PVA. About 0.15 g of powdered sample was shaken with 30 mL $NaHCO_3$ for 20 h. The contents were separated and the filtrate was collected. An aliquot of the solution was mixed with excess of 0.05*N* HCl and the CO_2 gas formed was boiled off and back titrated with std. NaOH.[18] Sulfonyl groups were calculated by substracting the amount of –COOH groups from the total amount of acidic groups present in P(AA-*co*-AAm-*co*-AMPS)-*g*-NC/PVA.

Characterization Methods

The X-ray diffraction (XRD) patterns of the DDS were recorded using an X'Pert Pro X-ray diffractometer using Cu Kα radiations. FTIR spectra were recorded with a Shimadzu FTIR

spectrometer using KBr pellet technique. Scanning electron microscopy (SEM) analysis was done using Philips XL 30 CP scanning electron microscope. Dynamic Light Scattering (DLS) measurements for the NC and NC/PVA were carried out in a laser scattering particle size distribution analyzer from Malvern Instruments. Water was used as the dispersant with refractive index 1.33 and viscosity 0.8872 cP. Concentration of AMO in solution was determined on a JASCO UV-vis (model V-530) spectrophotometer. All pH measurements were carried out on a Systronic model μ pH system 361-pH meter. A temperature controlled water bath shaker (Labline, India) with temperature variation of ±1°C was used for the equilibrium studies. Borosil glasswares were used throughout the experiment.

Swelling Characteristics

Swelling experiments were performed by immersing about 0.1 g of dried P(AA-*co*-AAm-*co*-AMPS)-*g*-NC/PVA in specified pH buffer solutions at 37°C for 4 h. The specified pH buffer solutions were prepared with KCl-HCl (pH from 1.0 to 2.0), $C_8H_5O_4K$-HCl (pH from 3.0 to 5.0), NaH_2PO_4-KH_2PO_4 (pH from 6.0 to 8.0). The weight of swollen samples was measured after drying superficially with filter paper. Swelling (%) was calculated by the following equation:[19]

$$\text{Swelling}\,(\%) = \frac{W_o - W_T}{W_T} \times 100 \qquad (1)$$

where W_o and W_T are the weights of the swollen and dry samples, respectively. The swelling kinetics was also performed, with solutions of KCl-HCl (pH 1.1) and Na_2HPO_4-KH_2PO_4 (pH 7.4) at 37°C. The effect of temperature on swelling was studied by varying temperature from 27 to 42°C at pH 7.4 and an equilibrium time of 4 h. The crosslinker and PVA concentration was changed from 0.05 to 0.40*M* and from 0.1 to 1.0 g, respectively for seeing the dependence of their amount on swelling. The NaCl concentration was varied from 0.01 to 0.2*M* for studying the effect of ionic strength upon swelling. The experiments were conducted twice for obtaining concordant values.

Drug Encapsulation Efficiency

Drug loading was carried out by adding predetermined amounts of AMO per gram to NC/PVA composite before graft copolymerization reaction. The drug encapsulation capacity of P(AA-*co*-AAm-*co*-AMPS)-*g*-NC/PVA was determined as follows. The drug loaded P(AA-*co*-AAm-*co*-AMPS)-*g*-NC/PVA was grounded to fine powder and 0.1 g of it was immersed into 50 mL Na_2HPO_4-KH_2PO_4 solution at pH 7.4 for 24 h under magnetic stirring. Then, the gel solution was centrifuged and the drug content in the supernatant solution was measured using UV-vis spectrophotometer at 272 nm.[20] The amount of drug was calculated from calibration curve that was obtained by absorbance of different concentrations of drug solution at 272 nm. The drug loading experiments were repeated three times and the average loading capacity of the P(AA-*co*-AAm-*co*-AMPS)-*g*-NC/PVA obtained from the repeated triplicate measurements was about 7.2 mg AMO per 100 mg P(AA-*co*-AAm-*co*-AMPS)-*g*-NC/PVA. i.e., 7.2%.

In Vitro Release of AMO

The *in vitro* drug release studies of the entrapped drug were carried out by placing the 0.1 g AMO-P(AA-*co*-AAm-*co*-AMPS)-*g*-NC/PVA into 50 mL KCl-HCl solution with pH 1.1 (simulative gastric pH) at 37°C in a water bath shaker. 3 mL of the solution were taken at predetermined time intervals and the concentration of AMO was measured at λ_{max} of 272 nm. The release studies were continued until no more change in the concentration of AMO in the solution. The same release experiments were repeated with Na_2HPO_4-KH_2PO_4 solution at pH 7.4 (simulated intestinal pH). The percentage of released AMO (%) in both cases was calculated by following the equation:

$$\text{Drug released}\,(\%) = \frac{C_t}{C_\infty} \times 100 \qquad (2)$$

where C_t and C_∞ are the concentration of drug released at time t and that of drug released completely, respectively. All the experiments were conducted in triplicates and the results were averaged. The maximum variation with batch adsorption data among triplicate values was 3.9%.

RESULTS AND DISCUSSION

Development of P(AA-*co*-AAm-*co*-AMPS)-g-NC/PVA and Its Characterization

Cellulose has been recommended as a suitable matrix for the delivery of drugs and hormones, owing to their biocompatible and biodegradable nature. Agricultural wastes such as wood sawdust have been found to be potential low-cost and easily available natural source for cellulose. The extraction of cellulose from saw dust not only reduces the economical value of the material, but also a remedial treatment for the removal of large number of timber industry waste. Saw dust basically contains cellulose, lignin, and polyoses. The acid-alkali treatment followed by bleaching produced white cellulose powder as the product. The acid hydrolysis of the cellulose powder, generated from saw dust, will break down its glucosidic linkage and produce a large number of free hydroxyl groups. Due to the large availability of hydroxyl groups exposed to surface, NC is generally hydrophilic in nature, which is highly desirable for making biocompatible materials. The properties of NC can further be increased by making it into composites. NC usually forms interpenetrating network structure upon association with PVA, which may hold large amounts of water and various molecules onto it. According to our experiments in laboratory, the physical stability, water holding capacity, drug encapsulation efficiency, and controlled drug release of NC/PVA composite was found to be very poor so as to making it into an efficient DDS. Therefore, chemical treatment such as graft copolymerization using different monomers onto NC/PVA composite was carried out to enhance the efficiency of the DDS.

P(AA-*co*-AAm-*co*-AMPS)-*g*-NC/PVA was synthesized by homogenous graft copolymerization of the AA, AAm, and AMPS onto the NC/PVA composite backbone using $K_2S_2O_8$ as a radical initiator and MBA as a crosslinking agent. The persulfate initiator on heating generates anionic radical SO_4^{-}. This anionic radical abstracts hydrogen from the hydroxyl groups of the NC/PVA to form macroradicals. In the presence of vinyl monomers, the microradical is added to the double bond of the monomer resulting in a covalent bond between the monomer and the NC/PVA. Although the three monomers form radicals, the more hydrophilic monomer with low molecular weight AA gets

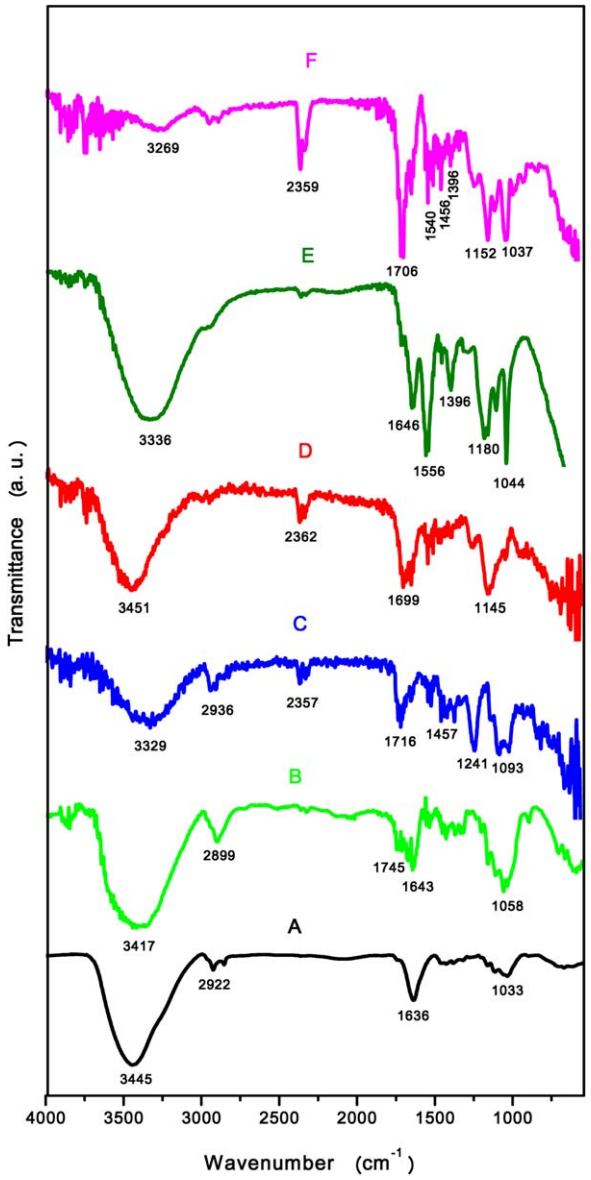

Figure 1. FTIR spectra of (A) Cellulose (B) NC (C) PVA (D) NC/PVA (E) AMO and (F) AMO-P(AA-*co*-AAm-*co*-AMPS)-*g*-NC/PVA. [Color figure can be viewed in the online issue, which is available at wileyonlinelibrary.com.]

attached first followed by AAm and AMPS. The presence of a cross-linking agent MBA in the system will create an interpenetrating polymer network with free and –COOH, -$CONH_2$, and –SO_3H functional groups at the chain end. The amount of sulfonyl and carboxyl functional group in P(AA-*co*-AAm-*co*-AMPS)-*g*-NC/PVA was estimated to be 2.03 meq g^{-1} and 1.49 meq g^{-1}, respectively.

The FTIR spectra of Cellulose, NC, PVA, NC/PVA, P(AA-*co*-AAm-*co*-AMPS)-*g*-NC/PVA, AMO-P(AA-*co*-AAm-*co*-AMPS)-*g*-NC/PVA are presented in Figure 1. The FTIR spectra of Cellulose shows the characteristic broad peak related to hydrogen bonded O—H stretching vibration at 3443 cm^{-1} and the peak at 2925 and 1033 cm^{-1} could be attributed to the C—H stretching and C—H bending of the CH_2 group. In 1635 and 668 cm^{-1}, there are signals corresponding to the C═O stretching of hemicelluloses and β-glycosidic linkage in cellulose, respectively. The band at 897 cm^{-1} is characteristic of glucosidic ring in cellulose structure. NC shows all the characteristic peaks of cellulose; however, its position slightly shifted which may be due to the removal of intramolecular H-bonding during acid hydrolysis.

PVA shows characteristic peaks of hydrogen bonded O—H stretching vibration at 3329 cm^{-1}. The peaks at 2936 and 1093 cm^{-1} indicate the C—H stretching and C—H bending of the CH_2 group. The NC/PVA contains both the peaks of NC and PVA with some shift in their position, confirms the interaction between NC and PVA during composite formation. AMO contains peaks at 3336 (-NH_2 stretching), 1646 (O—H stretching), 1396 (symmetric deformation of –CH_3 group), and 1180 cm^{-1} (sulfonate group), which confirm the structurally stable amoxicillin.

The characteristic absorption bands of the sulfonate group at 1163, 1039, and 590 cm^{-1}, respectively, were also observed in the spectrum of AMO-P(AA-*co*-AMPS)-*g*-NC/PVA. The

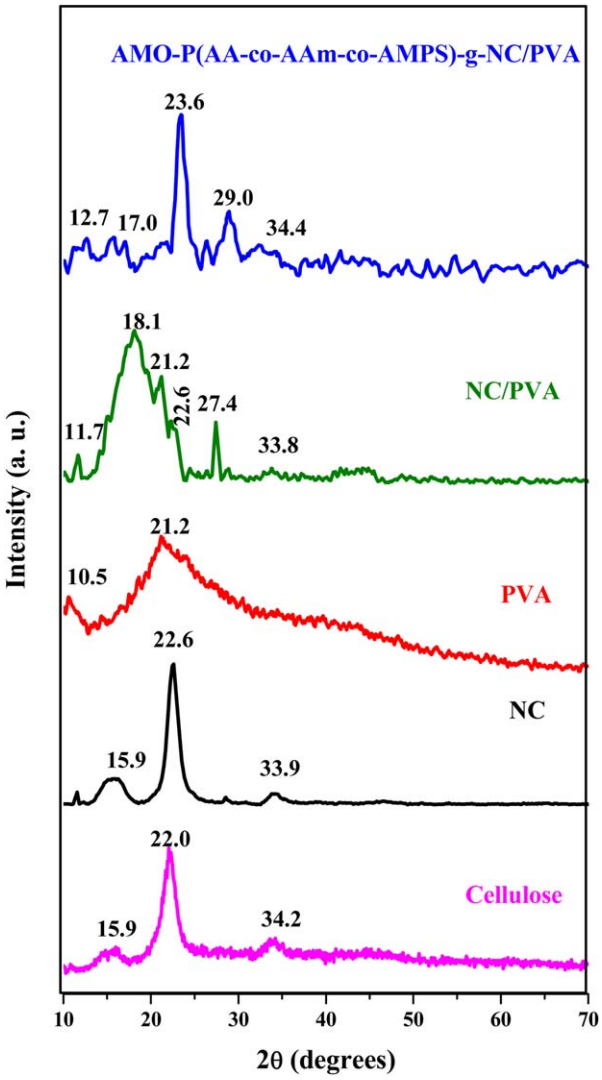

Figure 2. XRD patterns of cellulose, NC, PVA, NC/PVA, and AMO-P(AA-*co*-AAm-*co*-AMPS)-*g*-NC/PVA. [Color figure can be viewed in the online issue, which is available at wileyonlinelibrary.com.]

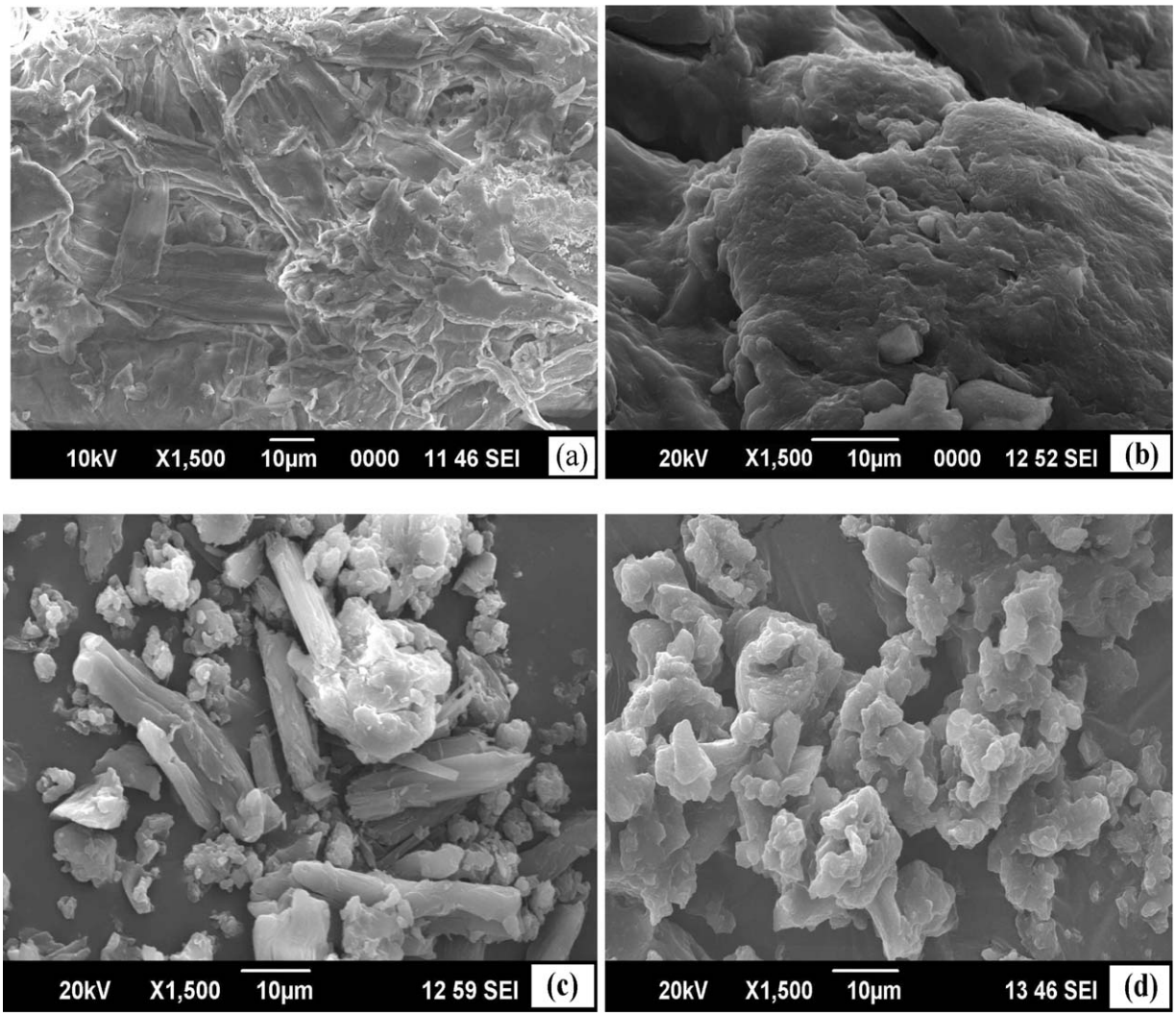

Figure 3. SEM Photographs of (a) Cellulose (b) NC (c) NC/PVA, (d) AMO-P(AA-*co*-AAm-*co*-AMPS)-*g*-NC/PVA.

presence of adsorption band at 1161 cm^{-1} indicates the presence of C—C vibrations. The peaks at 2939, 1540, 1391 cm^{-1} indicate the asymmetric stretching, asymmetric deformation and symmetric deformation of $–CH_3$ group. The presence of these characteristic bands confirms the graft copolymerization of NC/PVA with AA, AAm, and AMPS. The sample shows a new sharp adsorption peak at 1712 cm^{-1}, a characteristic of an ester carbonyl group. Shifting in the characteristic peak of O—H appeared in FTIR of AMO-P(AA-*co*-AMPS)-*g*-NC/PVA clearly confirms the existence of grafting. The presence of AA, AAm, and AMPS was confirmed by the vibration frequencies: 1672 cm^{-1} (C═O stretch), 3352/3182 (NH_2 stretch), 1610 cm^{-1} (NH_2 deformation), 1426 cm^{-1} (primary amides), 1244 cm^{-1} (asymmetric SO_2), 1078 (symmetric SO_2), and ~3000 cm^{-1} (OH stretch band for sulfonic acid).

Figure 2 shows the XRD patterns of cellulose, NC, PVA, NC/PVA, and AMO-P(AA-*co*-AAm-*co*-AMPS)-*g*-NC/PVA. The XRD pattern of cellulose shows peaks at 2θ values of 22.2° and 33.8° correspond to crystalline domain of cellulose structure. A broad hump at $2\theta = 15.9$○ reveals its amorphous nature. The peaks of NC retained its position as that of cellulose, however, they appeared even sharper which are indicative of a high degree of crystallinity in the structure, due to the partial removal of the amorphous regions during the acid hydrolysis treatment of cellulose.[21] The increase in broadness of the peak may be due to the small particle size and induced strain during the conversion to nanocrystals.

The particle size of NC was calculated from the full width at half maximum (FWHM) by applying Debye–Scherrer formula:

$$D = \frac{K\lambda}{\beta \cos\theta} \tag{3.1}$$

where D is the average nanocrystal diameter in Å, K is the shape factor (0.9-1), λ is the X-ray wavelength, β is the size induced line broadening (FWHM), and θ is the diffraction angle. The particle size of NC was found to be 25.0 nm and this small particle size will increase the surface area and grafting

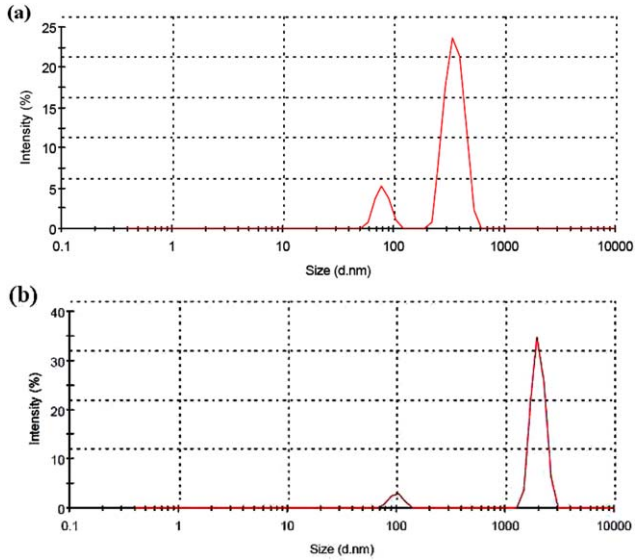

Figure 4. Particle size distribution of NC (a) and NC/PVA (b). [Color figure can be viewed in the online issue, which is available at wileyonlinelibrary.com.]

efficiency, which in turn may increase the drug encapsulation efficiency. The broader peaks also support their smaller grain size.[22]

PVA shows two characteristic peaks at 11.7 and 21.7○. NC/PVA exhibits both the peaks of NC and PVA, with slight modification, which suggests that an interaction has been occurred during composite formation. The presence of new peaks and decreased crystallinity of AMO-P(AA-*co*-AAm-*co*-AMPS)-*g*-NC/PVA confirms the polymerization reaction upon NC/PVA composite.

In this study, SEM (Figure 3) was used to probe the change in morphological features of Cellulose, NC, NC/PVA, and AMO-P(AA-*co*-AMPS)-*g*-NC/PVA. Cellulose seems to be fibrous in nature, while, NC looks fluffy and behaves like a gel, which may be due to the increased hydrophilicity. This gel structure is suitable for the drug delivery vehicles. NC/PVA combines both the nature of NC and PVA. Nanocellulose fibres appear to be dispersed in a PVA matrix. AMO-P(AA-*co*-AMPS)-*g*-NC/PVA clearly indicates that polymers have been adhered on the NC/PVA composite.

Dynamic Light Scattering (DLS) Studies

Dynamic Light Scattering (DLS) studies (Figure 4) were carried out to measure the particle size of NC and NC/PVA. NC shows two peaks with average particle size of 80.3 and 358.2 nm, while NC/PVA shows two peaks having average particle size of 100.9 and 203.6 nm. The dimensions of the cellulose nanocrystals closely match previously reported work of several authors.[23,24] The polydispersity index (PDI) of NC and NC/PVA was determined to be 0.522 and 0.897, respectively. PDI measurement indicates the width of the particle size distribution and shows the value zero for a highly mono-dispersed sample and 1 or more for a highly poly-dispersed sample. Thus the PDI values obtained for the NC and NC/PVA dispersions indicates a high degree of monodispersity for NC and some degree of polydispersity for NC/PVA.

Swelling Studies

The presence of water at the surface of hydrogels results in low frictional forces, which is a desirable property in developing biocompatible materials.[25] The extent of swelling will generally dictate the rate at which the drug released. As swelling increases, drug release will be more diffusion-controlled or erosion-controlled for water-soluble and water-insoluble drugs, respectively. When the hydrogel is soaked in water, the water penetrates into the gel in the form of a front, and shifts from surface to the core. Earlier workers have described the role of swelling in the release of amoxicillin from polyionic complexes.[26] Concerning this aim, we also conduct swelling measurements of the newly developed DDS. The hydrogel can swell at different rates depending on many factors; and some of them are discussed below.

Effect of pH. It was observed that with increase in pH from 1.0 to 8.0, swelling % also increases (Figure 5). The pK_a of the PAA is around 4.5 and that of PAMPS is around 2.5. When pH is less than pK_a, the H^+ ion strength will be high, which will effectively suppress the ionization of –COOH and $–SO_3H$ groups. So, at acidic pH, the gel is neutral due to the protonation of carboxylate and sulfonate anions and flexibility of the polymeric chain is rather low. Also, at low pH, the acidic protons of carboxyl and sulfonyl groups of PAA and PAMPS interact with the nitrogen or oxygen of amide group from PAAm through hydrogen bonding, and such complexation results in the shrinkage of the hydrogels. With increase in pH, PAA and PAMPS become ionized and the resulting decomplexation leads to swelling of hydrogels. Besides, the ionization of both –COOH and $-SO_3H$ enhanced gradually with increase in pH and swelling increases due to the increased anion-anion repulsive forces. Increase in the anion density also results in high swelling capacity. It is due to the fact that with increase in anionic density, hydrophilicity of the hydrogel increases, the interaction between water and hydrogel will increase too, which facilitates

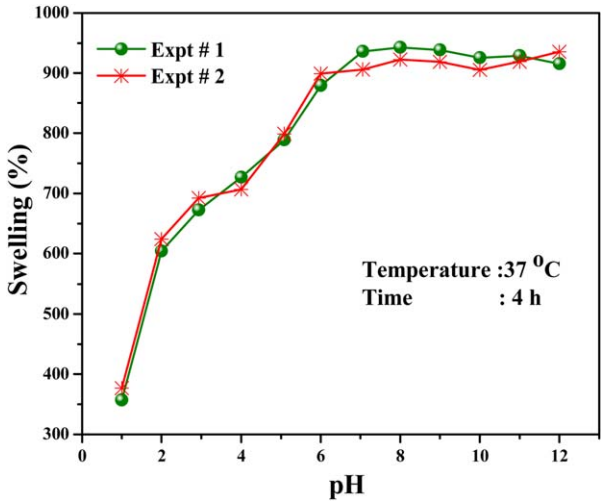

Figure 5. Swelling (%) as a function of solution pH. [Color figure can be viewed in the online issue, which is available at wileyonlinelibrary.com.]

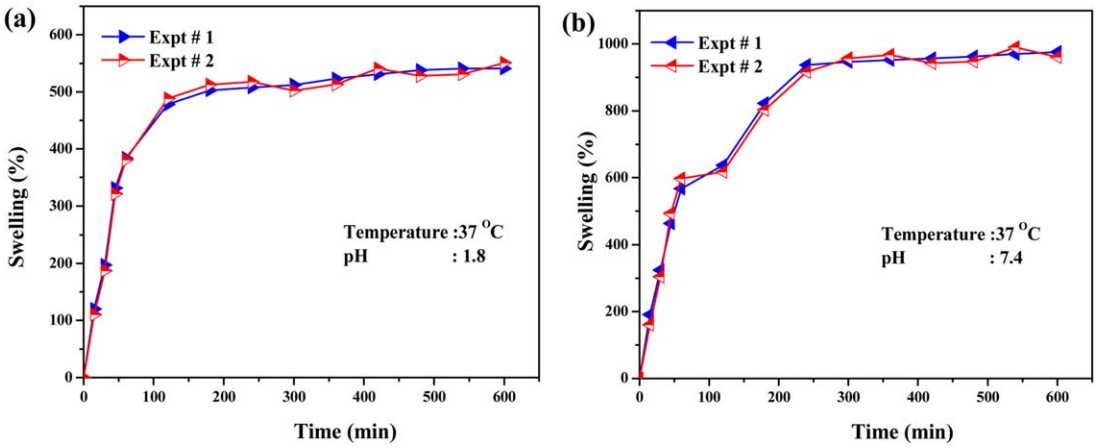

Figure 6. Swelling kinetic profiles of P(AA-*co*-AAm-*co*-AMPS)-*g*-NC/PVA with time at pH 1.8 and 7.4. [Color figure can be viewed in the online issue, which is available at wileyonlinelibrary.com.]

water diffusion and leads to greater swelling. However, this pH trend can be exploited in the swelling controlled releasing systems in intestines. Kim et al. used anionic hydrogels as oral protein delivery carriers because of their pH-dependent swelling behavior.[27] Isik and Dogantekin prepared random copolymers of AAm and N-vinylimidazole using redox system which shows the highest equilibrium swelling in basic medium.[28]

Swelling Kinetics. The dependency of swelling capacity with contact time was studied and the results were depicted in Figure 6. As shown in figure, swelling % increases with increase in time upto ~4.0 h, after that tends to equilibrium. The greater extent of swelling at pH 7.4 compared with that at pH 1.8 may be more likely due to enhanced electrostatic repulsion between the neighbouring COO- and SO_3^- ions. The neutral monomer AAm which resides between AA and AMPS increase the spacing for accommodating water and solute molecules. However, at acidic pH < 2, the majority of the acid groups exists in undissociated forms and led to decreased swelling. Generally, the existence of hydrophilic moieties such as hydroxyl and carboxylic groups tends to increase the hydrophilicity of a polymeric material and consequently increases its swelling values attained equilibrium.[29]

Also, it was observed that SAPC retains its swelling value almost constant even after 10 days (figure not shown), which suggests that P(AA-*co*-AAm-*co*-AMPS)-*g*-NC/PVA structure is mechanically strongest and can be used for long-term delivery devices.

Effect of Temperature. To know the influence of temperature on the swelling behavior, swelling experiments were conducted at temperatures between 27 and 42∘C (Figure 7). When the temperature was increased from 27 to 42∘C, the swelling ratio was also increased. This positive swelling change of P(AA-*co*-AAm-*co*-AMPS)-*g*-NC/PVA with temperature indicating the occurrence of upper critical solution temperature (UCST) behavior. Similar behavior has been reported earlier with anionic hydrogels.[30] The hydrogels based on AAm and N-vinylimidazole exhibited a high degree of swelling at higher temperatures.

Effect of Crosslinker Concentration. The hydrogel characteristics, including the swelling properties and strength, can be modulated by the amount of cross-linking agent. The dependence of swelling ratio with respect to crosslinker concentration is represented in Figure 8, which suggests a decreased swelling with increase in crosslinker density. Similar results were observed in previous literatures.[31] The relationship between swelling (s) and concentration of crosslinker (C) can be stated as:

$$S = kC^{-n} \tag{4}$$

Where k and n are the constant values for an individual hydrogels. Here the values of k and n were found to be 2.73 and 0.36, respectively.

For a noncrosslinked hydrogel, hydrogel molecules will eventually dissolve in water and occupy the whole volume, as already occupied by water. As the crosslinking density increases, hydrogel molecules behave similar to semi-solid molecules with less entropy. At higher concentrations, the extent of crosslinking of the polymer network will increase and hydrogel molecules behave like a solid with minimum entropy, which cannot be expanded to hold a large quantity of water.[25]

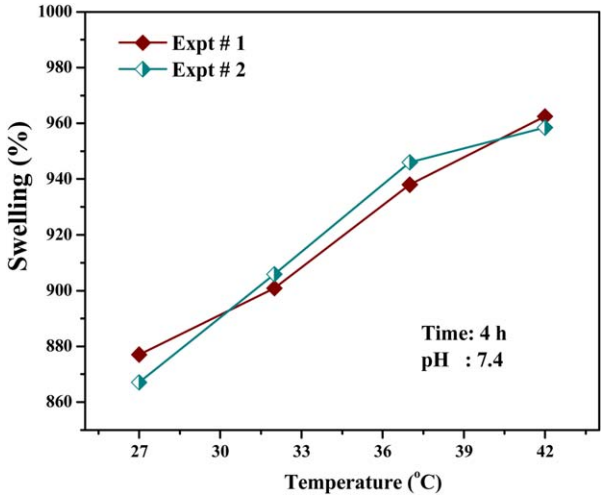

Figure 7. Swelling (%) as a function of temperature. [Color figure can be viewed in the online issue, which is available at wileyonlinelibrary.com.]

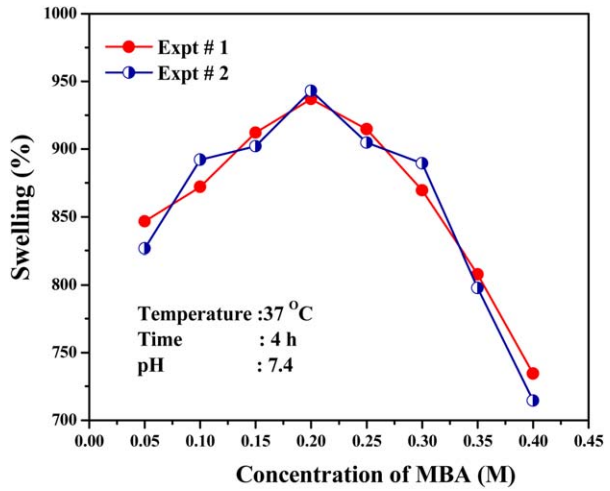

Figure 8. Swelling (%) as a function of MBA concentration. [Color figure can be viewed in the online issue, which is available at wileyonlinelibrary.com.]

Effect of PVA Concentration. The effect of PVA concentration on the swelling is shown in Figure 9. As the weight of PVA increases from 0.1 to 1.0 g, swelling capacity also increase from 0.1 to 0.65 g and decreases after 0.65 g of addition. As the weight of PVA increased from 0.1 to 0.65 g, the active sites can react easily with monomers. Increasing the PVA content beyond 0.65 g, results in a high viscosity of the medium and decreased the diffusion of monomers to active sites to produce crosslinked hydrogels.

Effect of Ionic Strength. As shown in Figure 10, the swelling capacity of the SAPC in salt (NaCl) solution was decreased with increasing the salt concentration. Swelling values for all anionic hydrogels in saline water is reported to be decreased concerning with distilled water. This undesired swelling loss may be attributed to the charge screening effect of the cations leading to the reduction of osmotic pressure, the driving force for swelling between the SAPC and the aqueous phases as explained by Pourjavadi and Mahdavinia.[32] The increased electrostatic attraction between anionic sites of polymer chains and cations (Na^+) may also increase in the ionic crosslinking degree and subsequent loss of swelling. Generally, ionic hydrogel chains behave like solid in high salt concentrations and changes to semi-solid molecules in low salt concentrations, respectively. Hydrogels do not swell appreciably in the presence of electrolytes salts due to ex-osmosis in the presence of salts.[32] The salt sensitivity factor, f (dimensionless) may be expressed as:

$$f = 1 - (S_s / S_w) \quad (5)$$

where S_s is swelling given in a given fluid (salt solution) and S_w is swelling in distilled water. The f factor in the present case is found to be 0.026, 0.069, 0.112, 0.186, and 0.276 when the salt concentrations were 0.01, 0.05, 0.1, 0.15, and 0.2*M*, respectively, which is lower than the fully synthetic hydrogels, and can be ascribed as its lower salt sensitivity. However, the decrease in swelling with increase in salt concentration can be explained as follows. At low ionic strengths, the concentration of bound charges within the hydrogel network exceeds the concentration of salt in the external solutions; a large ion-swelling pressure causes the hydrogel to expand, thereby lowering the concentration of ions within the hydrogel. As the external salt concentration rises, the difference between the internal and external ion concentration decreases and the hydrogel deswells. The hydrogel continues to deswell with increasing external salt concentration until the mobile-ion concentrations inside and outside are approximately equal.[33]

Drug Release Profiles

When drug bearing SAPCs comes in contact with aqueous medium, water penetrates into the system and dissolves the drug. The dissolved drug dissolves out of the delivery systems to the surrounding aqueous medium, due to Brownian motion of the drug molecules. According to earlier reports, the drug will be released from a swellable hydrogel through diffusion, degradation or both depending on the level of swelling and

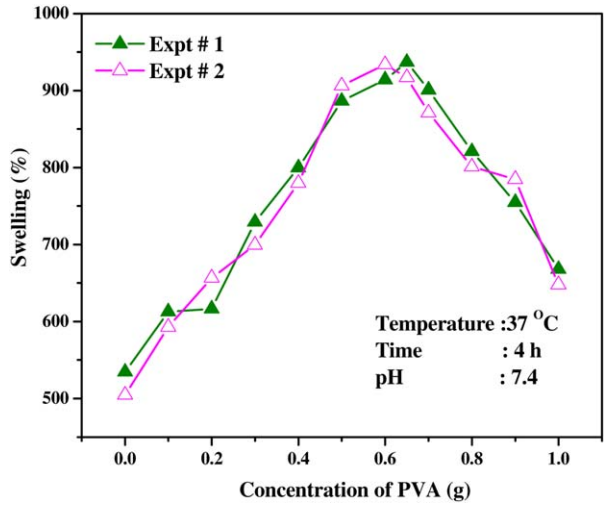

Figure 9. Swelling (%) as a function of PVA concentration. [Color figure can be viewed in the online issue, which is available at wileyonlinelibrary.com.]

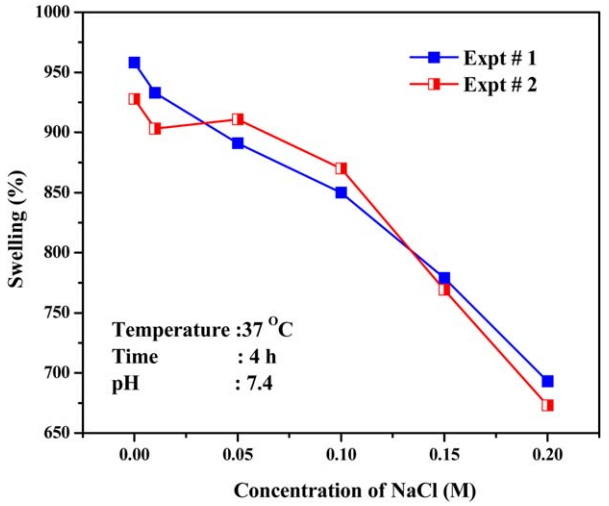

Figure 10. Swelling (%) as a function of NaCl concentration. [Color figure can be viewed in the online issue, which is available at wileyonlinelibrary.com.]

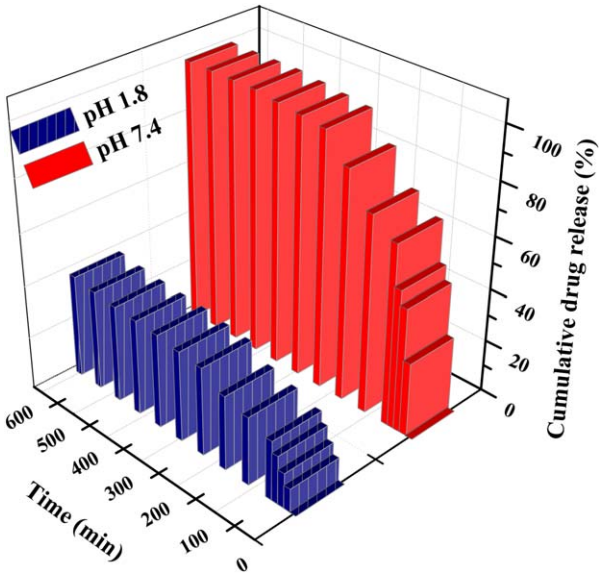

Figure 11. *In vitro* release profile of AMO at pH 1.8 and 7.4. [Color figure can be viewed in the online issue, which is available at wileyonlinelibrary.com.]

solubility of the drug. If the drug is water soluble, diffusion will be the primary mechanism. Here the drug, AMO is water soluble and therefore the release from the swellable hydrogel may be through diffusion of drug molecules. However, the diffusion of the drug molecules through the SAPCs may be affected by the stimuli-response property of the SAPC and has been used successfully as drug delivery vehicles. The following sections discuss with the common stimuli-responsive factors which optimize the release of drug at a suitable environment.

Effect of pH on Drug Release. Here, we consider two buffer solutions of pH 1.1 (KCl-HCl) and pH 7.4 (Na_2HPO_4-KH_2PO_4) for releasing AMO into the stomach and intestine, respectively. The percentage drug release (%) of AMO calculated using eq. (2) at pH 1.1 and 7.4, at 37○C is depicted in Figure 11. The release % was found to be 33.7 and 97.0 for a pH of 1.1 and 7.4, respectively at 4 h. This behavior indicates that AMO release from P(AA-*co*-AAm-*co*-AMPS)-*g*-NC/PVA is pH dependent. The release percentage of AMO was higher in the alkaline medium than in the acidic medium. The increase in drug release at higher pH may be attributed to the increased swelling capacity of the SAPC with increase in pH, which leads to the ionization of both –COOH and $–SO_3H$ groups. This parallel behavior indicates that drug release mechanism is swelling-controlled.

Release Kinetics in Simulative Gastric and Intestinal Fluids. Release kinetics of AMO from P(AA-*co*-AAm-*co*-AMPS)-*g*-NC/PVA at pH 1.8 and 7.4 is presented in Figure 11. As seen in figure, the release % was increased with increase in time and a maximum was achieved at 4 h. UV-visible spectra (Figure 12) confirms the time-dependent release of AMO from P(AA-*co*-AAm-*co*-AMPS)-*g*-NC/PVA matrix at pH 7.4. To investigate more precisely the effect of interpolymer complex formation on the release of AMO, the results were analyzed according to the Peppas' potential equation:[34]

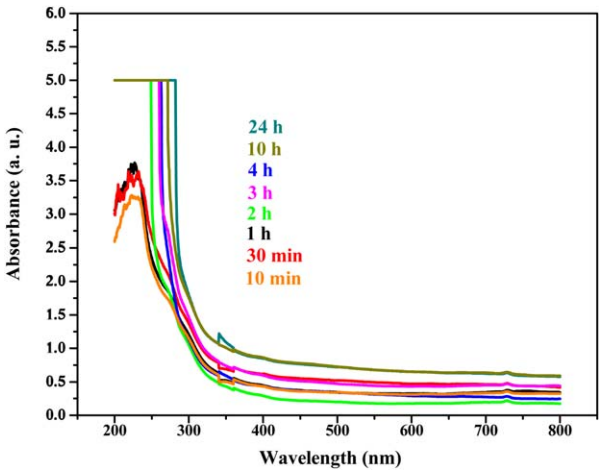

Figure 12. UV-visible spectra of time-dependent release of AMO at pH 7.4. [Color figure can be viewed in the online issue, which is available at wileyonlinelibrary.com.]

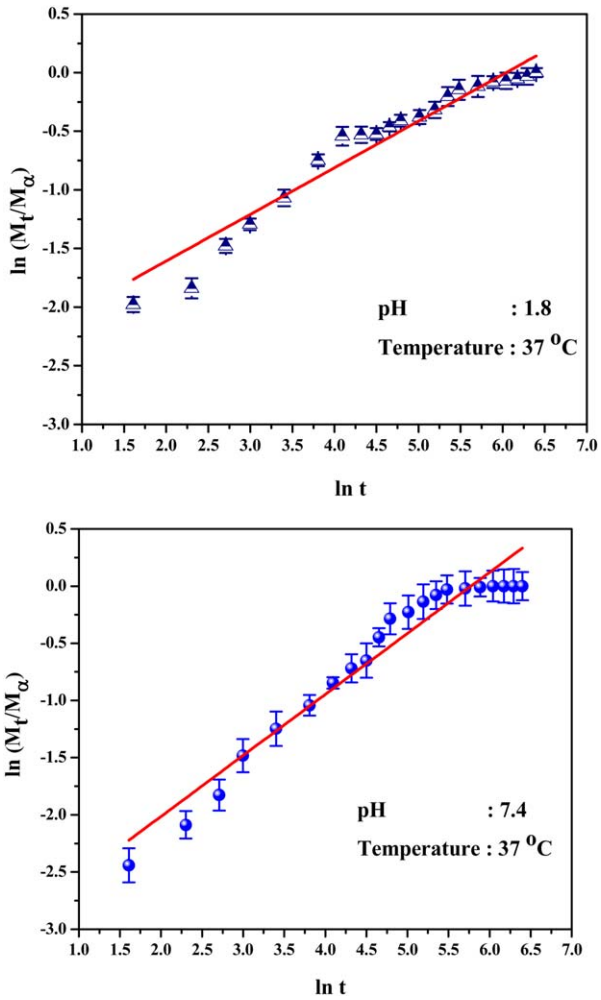

Figure 13. Peppa's plots for the release of AMO from P(AA-*co*-AAm-*co*-AMPS)-*g*-NC/PVA at pH 1.8 and 7.4. [Color figure can be viewed in the online issue, which is available at wileyonlinelibrary.com.]

Table I. Kinetic Parameters for AMO Release from P(AA-*co*-AAm-*co*-AMPS)-*g*-NC/PVA

pH	Temperature	*k*	*n*	R^2
1.8	37°C	−2.402	0.397	0.932
7.4	37°C	−3.080	0.533	0.950

$$M_t = M_\infty k t^n \quad (6)$$

where M_t and M_∞ are the amount of AMO released (%) at time t and that of released completely, respectively. k is the apparent release rate (%/h) and n is the diffusion exponent, which characterizes the diffusion mechanism. The drug release parameters, n and k are obtained from the slope and intercept of plot of ln (M_t/M_∞) versus ln t (Figure 13). It was observed that the plot of ln (M_t/M_∞) versus ln t appears to be straight line, and the parameters are given in Table I.

The n value can be used to identify the release mechanisms. When $n = 0.43$, Fickian diffusion is dominant and in this case the diffusion of drug molecules plays an important role during release process.[35] When $n = 0.85$, a swelling controlled release occurs and the release process of drug is limited by the expanding of the polymer segment to accommodate penetration.[36] Values of n between 0.43 and 0.85 are an indication of non-Fickian or anomalous drug diffusion mechanism where both diffusion and swelling control the overall rate of release of drug.[37]

The n value (0.533) obtained from the release kinetic model for this study at a pH 7.4 medium shows that the drug release from the DDS is a combined process of drug diffusion and polymer matrix relaxation.[38] It means that at pH 7.4, the drug release kinetics of the controlled release matrix can be determined by diffusion process of drug partially through the swollen polymer network and partially through the water-filled pores and channels in the network structure, and the erosion of polymer matrix.[39] However, the value of n (0.397) at pH 1.8 clearly shows that drug release is only diffusion controlled. The poor swelling as compared with pH 7.4 supports this result. The k-values range between −3.08 and −2.40, indicating mild-type of interactions between the drug and the polymer matrices. Smaller values of k indicated the prolonged release of drug from the drug carrier. Thus, the value of k and n suggests the release of AMO from P(AA-*co*-AAm-*co*-AMPS)-*g*-NC/PVA will be delayed and controllable.

CONCLUSIONS

Helicobacter pylori has been recognized as a major pathogen with worldwide distribution and AMO is proved to be most active against *Helicobacter pylori*. In this work, we have synthesized a stimuli-responsive drug carrier, P(AA-*co*-AAm-*co*-AMPS)-*g*-NC/PVA for the gastrointestinal release of AMO. The physicochemical properties of the P(AA-*co*-AAm-*co*-AMPS)-*g*-NC/PVA were investigated. The swelling capacity of P(AA-*co*-AAm-*co*-AMPS)-*g*-NC/PVA was varying with change in pH, contact time, temperature, crosslinker density, PVA concentration, and ionic strength. Drug encapsulation efficiency of the P(AA-*co*-AAm-*co*-AMPS)-*g*-NC/PVA was optimized. Drug release was found to be easier in intestine rather than gastric region, as evident from the *in vitro* drug release studies. The drug release kinetics follows non-Fickian mechanism, where diffusion and polymer relaxation controls the drug release. Thus the present investigation represents P(AA-*co*-AAm-*co*-AMPS)-*g*-NC/PVA as a drug carrier for the eradication of *Helicobacter pylori*.

ACKNOWLEDGMENTS

The authors acknowledge the University Grants Commission, New Delhi for financial support of the research activities, in the form of Major Research Project (MRP F. No. 37–425/2009 (SR), related to the production of cellulose-based hydrogels for biomedical applications.

REFERENCES

1. Pandit, V.; Suresh, S.; Joshi, H. *Int. J. Pharma. Biosci.* **2010**, *1*, 1.
2. Forman, D.; Webb, P.; Parsonnet, J. H. *Lancet* **1994**, *343*, 243.
3. Umamaheshwari, R. B.; Ramteke, S.; Jain, N. K. *AAPS Pharm. Sci. Technol.* **2004**, *5*, 1.
4. Nagahara, N.; Akiyama, Y.; Nako, M.; Tada, M.; Kitano, M.; Ogawa, Y. *Antimicrob. Agents Chemother.* **1998**, *42*, 2492.
5. Wang, J.; Tauchi, Y.; Deguchi, Y.; Morimoto, K.; Tabata, Y.; Ikada, Y. *Drug Deliv.* **2000**, *7*, 237.
6. Liu, Z.; Lu, W.; Qian, L.; Zhang, X.; Zeng, P. L.; Pan, J. *J. Control. Release* **2005**, *102*, 135.
7. Patel, M. P.; Patel, R. P.; Patel, J. K. *J. Pharm. Pharmaceut Sci.* **2010**, *13*, 536.
8. Efentakis, M.; Politis, S. *Eur. Polym. J.* **2006**, *42*, 1183.
9. Sannino, A.; Demitri, C.; Madaghiele, M. *Materials* **2009**, *2*, 353.
10. El-Hag Ali, A.; Abd El-Rehim, H.; Kamal, H.; Hegazy, D. *J. Macromol. Sci. Pure Appl. Chem.* **2008**, *45*, 628.
11. Gartiser, S.; Wallrabenstein, M.; Stiene, G. *J. Environ. Polym. Degrad.* **1998**, *6*, 159.
12. Tang, X.; Alavi, S. *Carbohydr. Polym.* **2011**, *85*, 7.
13. Kvien, I.; Oksman, K. *Appl. Phys. A* **2007**, *87*, 641.
14. Ibrahim, M. M.; El-Zawawy, W. K.; Nassar M. A. *Carbohydr. Polym.* **2010**, *79*, 694.
15. Khare, A. R.; Peppas, N. A. *J. Biomater. Sci. Polym. Ed.* **1993**, *4*, 275.
16. Brannon-Peppas, L.; Peppas, N. A. *Biomaterials* **1990**, *11*, 635.
17. Anirudhan, T. S.; Rejeena, S. R. *Carbohydr. Polym.* **2013**, *93*, 518.
18. Shibi, I. G.; Anirudhan, T. S. *Ind. Eng. Chem. Res.* **2002**, *41*, 5341.
19. Pal, K.; Banthia, A. K.; Majumdar, D. K. *AAPS Pharm. Sci. Technol.* **2007**, *8*, E142.
20. Patel, J. K.; Patel, M. M. *Current Drug Deliv.* **2007**, *4*, 41.
21. Alemdar, A.; Sain, M. *Bioresour. Technol.* **2008**, *99*, 1664.

22. Anirudhan, T. S.; Rejeena, S. R. *Chem. Eng. J.* **2012**, *187*, 150.
23. Bondeson, D.; Mathew, A.; Oksman, K. *Cellulose* **2006**, *13*, 171.
24. Filson, P. B.; Dawson-Andoh, B. E.; Schwegler-Berry, D. *Green Chem.* **2009**, *11*, 1808.
25. Omidian, H.; Park, K. *J. Drug Deliv. Sci. Technol.* **2008**, *18*, 83.
26. De la Torre, P. M.; Enobakhare, Y.; Torrado, G.; Torrado, S. *Biomaterials* **2003**, *24*, 1499.
27. Kim, B.; LaFlamme, K.; Peppas N. A. *J. Appl. Polym. Sci.* **2003**, *89*, 1606.
28. Isik, B.; Dogantekin, B. *J. Appl. Polym. Sci.* **2005**, *96*, 1783.
29. El-Sherbiny, I. M.; Smyth, H. D. C. *Carbohydr. Polym.* **2010**, *81*, 652.
30. Ekici, S.; Saraydin, D. *Polym. Int.* **2007**, *56*, 1371.
31. Mohammad, S.; Fatemeh, S. *Res. J. Chem. Environ.* **2012**, *16*, 125.
32. Pourjavadi, A.; Mahdavinia, G. R. *Turk. J. Chem.* **2006**, *30*, 595.
33. Xu, S.; Wu, R.; Huang, X.; Cao, L.; Wang, J. *Turk. J. Chem.* **2010**, *34*, 739.
34. Korsmeyer, R. W.; Gurny, R.; Doelker, E.; Buri, P.; Peppas, N. A. *Int. J. Pharm.* **1983**, *15*, 25.
35. Falk, B.; Garramone, S.; Shivkumar, S. *Mater. Lett.* **2004**, *58*, 3261.
36. Hopkinson, I.; Jones, R. A. L.; Black, S.; Lane, D. M.; McDonald, P. *J. Carbohydr. Polym.* **1997**, *34*, 39.
37. Jin, S.; Liu, M.; Chen, S.; Gao, C. *Mater. Chem. Phys.* **2010**, *123*, 463.
38. Tapia, C.; Corbalan, V.; Costa, E.; Gai, M. N.; Yazdani-Pedram, M. *Biomacromolecules* **2005**, *6*, 2389.
39. Chen, S.; Liu, M.; Jin, S.; Wang B. *Int. J. Pharm.* **2008**, *349*, 180.